A theory of network alteration for the Mullins effect

Gilles Marckmann, Erwan Verron, Laurent Gornet, Gregory Chagnon, Pierre Charrier, P. Fort

A theory of network alteration for the Mullins effect

G. Marckmann[a,*], E. Verron[a], L. Gornet[a], G. Chagnon[a], P. Charrier[b], P. Fort[b]

[a]Laboratoire de Mécanique et Matériaux, École Centrale de Nantes, BP 92101, 44321 Nantes Cedex 3, France
[b]Groupe Trelleborg, Société Modyn, Service Recherche et Innovations, Zone Industrielle Nantes Carquefou BP 419, 44474 Carquefou Cedex, France

Abstract

This paper reports on the development of a new network alteration theory to describe the Mullins effect. The stress-softening phenomenon that occurs in rubber-like materials during cyclic loading is analysed from a physical point of view. The Mullins effect is considered to be a consequence of the breakage of links inside the material. Both filler-matrix and chain interaction links are involved in the phenomenon. This new alteration theory is implemented by modifying the eight-chains constitutive equation of Arruda and Boyce (J. Mech. Phys. Solids 41 (2) (1993) 389). In the present method the parameters of the eight-chains model, denoted C_R and N in the bibliography, become functions of the maximum chain stretch ratio. The accuracy of the resulting constitutive equation is demonstrated on cyclic uniaxial experiments for both natural rubbers and synthetic elastomers.

Keywords: A. Rubber material; B. Stress softening; Polymer network; Finite strain; Constitutive behaviour

1. Introduction

In recent years, the industrial competition has led the automotive companies to validate their products numerically. The prediction of the fatigue life of rubber-like and elastomeric parts, such as engine mounts, has become necessary. An essential prerequisite for the finite element simulation of this phenomenon is a well-established knowledge of the material behaviour.

* Corresponding author. Fax: 33-2-40-25-73.
E-mail address: gilles.marckmann@ec-nantes.fr (G. Marckmann).

Elastomers exhibit a highly non-linear behaviour characterized by three main phenomena: a non-linear elastic behaviour under static load; a rate-dependent or viscoelastic behaviour with hysteresis under cyclic loading; and a so-called Mullins effect, which can be described as a stress-softening phenomenon of the material after a primary load. Another phenomenon, the Payne effect, involves the thixotropic behaviour under dynamic loading (Lion, 1998).

The aim of this paper is to present a new network model for the Mullins effect, based on physical interpretations of the phenomenon. A theoretical network alteration approach is developed in order to adapt the classical eight-chains model of Arruda and Boyce (1993). It is shown that the parameters of this model can be simply replaced by functions of the maximum stretch ratio in order to incorporate the Mullins effect in the constitutive equation. In this study, only static behaviour is considered, and viscoelastic effects are not taken into account.

In Section 2, classical hyperelastic constitutive equations are recalled, and their phenomenological or physical origins are highlighted. Emphasis is placed on the network chains models. Section 3 is devoted to the presentation of the Mullins effect. Macroscopic observations, physical interpretations and constitutive modelling are reviewed. Our network alteration theory is presented in the Section 4. A modified version of the Arruda and Boyce eight-chains model is derived. The corresponding parameters are numerically identified using uniaxial experimental results for NR and SBR. Finally, concluding remarks are given in Section 5.

2. Rubber elasticity

2.1. Generalities

Rubber-like materials are classically considered isotropic, incompressible and hyperelastic. They are defined by a strain energy function W, and each particular model is described by a special form of this function (Treloar, 1976). The major challenge is the construction ofW according to phenomenological and physical considerations.

Once given the form ofW, the Cauchy stress tensor can be obtained by

$$\boldsymbol{\sigma} = -\mathrm{pI} + 2\,\mathrm{B}\,\frac{\partial W}{\partial \mathbf{B}}. \tag{1}$$

where $\mathbf{B}$ is the left Cauchy–Green stretch tensor and p stands for the hydrostatic pressure introduced by the incompressibility assumption. Moreover, W is generally expressed as a function of the first and second strain invariants, respectively, given by

$$I_1 = \operatorname{tr}\mathbf{B} \quad \text{and} \quad I_2 = \tfrac{1}{2}[I_1^2 - \operatorname{tr}(\mathbf{B}^2)] \tag{2}$$

or as a function of the principal stretch ratios (the square roots of the eigenvalues of $\mathbf{B}$): λ_1, λ_2 and λ_3. Note that the third invariant of $\mathbf{B}$ is considered equal to 1 due to incompressibility. Consequently, the principal stretch ratios are related together by

$$\lambda_1\lambda_2\lambda_3 = 1. \tag{3}$$

The forms of the strain energy function W have been examined by many authors since the 1940s. They are, for a large part, derived using phenomenological or empirical approaches, as functions of the strain invariants I_1 and I_2 (Mooney, 1940; Rivlin and Saunders, 1951; Gent and Thomas, 1958; Hart-Smith, 1966) or of the principal stretch ratios $(\lambda_i)_{i=1;3}$ (Valanis and Landel, 1967; Ogden, 1972). All of these constitutive equations are based on experimental observations and mathematical developments. No physical considerations are invoked to justify the various expressions of W.

2.2. Network constitutive equations

The second approach used to develop stress–strain relations for rubber-like materials is based on network physics. The polymer is considered as a network of long flexible chains randomly oriented and joined together by chemical cross-links. According to the statistical theory of rubber elasticity, the deformation is associated with a reduction of entropy in the network. Details on this subject can be found in Treloar (1975).

2.2.1. Gaussian statistics model

At the same time as the phenomenological Mooney model was proposed, Treloar used Gaussian statistics applied on the chains network to describe the macroscopic behaviour of rubber-like materials. These physical considerations lead to the neo-Hookean constitutive equation (Treloar, 1943). The corresponding strain energy function is given by

$$W = \tfrac{1}{2} nkT(I_1 - 3), \tag{4}$$

where n denotes the average number of polymer chains per unit of volume, k is the Boltzmann constant and T is the absolute temperature. This model agrees well with experiments for small strains.

2.2.2. Non-Gaussian statistics models

In order to overcome the limitations of the previous model, authors use the more complex non-Gaussian statistics theory to describe molecular chains deformations.

2.2.2.1. Single-chain elasticity. In 1942, Kuhn and Grün used the non-Gaussian statistics theory to describe the stretching limit of chains (Kuhn and Grün, 1942). This approach is based on the random walk statistics of ideal phantom chain detailed in Doi (1996). Consider a molecular chain composed by N monomer segments of length l; its average unstretched length is $\sqrt{N}l$ and its total stretched length is Nl. Consequently, the limiting extension ratio is $\sqrt{N}$. Moreover, as shown by Kuhn and Grün, the strain energy function of the chain, w, can be written in the following form:

$$w = NkT\left[\frac{\lambda}{\sqrt{N}}\beta + \ln\frac{\beta}{\sinh\beta}\right] \tag{5}$$

with $\beta = \mathscr{L}^{-1}(\lambda/\sqrt{N})$, and where $\mathscr{L}^{-1}$ is the inverse Langevin function defined by $\mathscr{L}(x) = \coth(x) - 1/x$. Thus, the true stress in a single chain is obtained by derivation

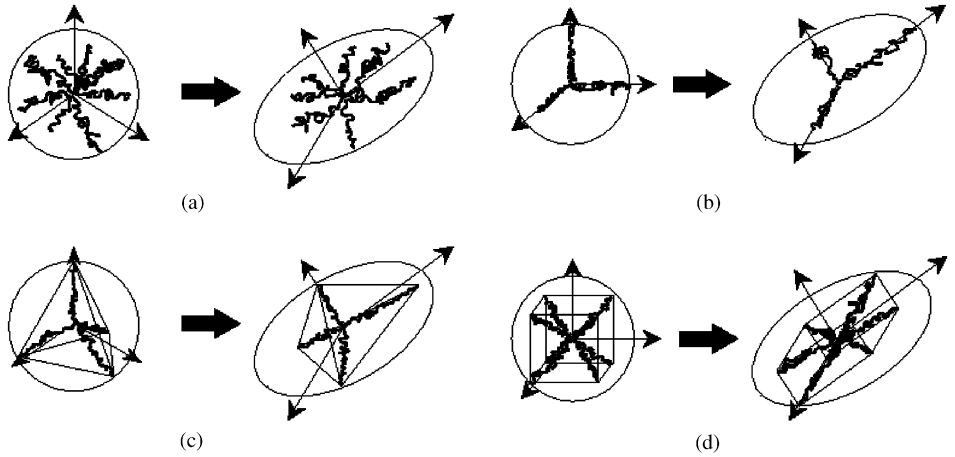

Fig. 1. Description of the non-Gaussian network models: (a) full network, (b) three chains, (c) four chains, (d) eight chains.

of w with respect to the extension:

$$\sigma = \lambda \frac{\partial w}{\partial \lambda} = \lambda kT\sqrt{N}\,\mathscr{L}^{-1}\left(\frac{\lambda}{\sqrt{N}}\right). \tag{6}$$

2.2.2.2. Full network model. Treloar and Riding (1979) considered a unit sphere of the material in which the chains are randomly oriented. Fig. 1(a) depicts the geometry of the problem in the undeformed and deformed states. The stress in Eq. (6) is numerically integrated on the sphere to obtain the response of the network under uniaxial or biaxial extensions. More recently, Wu and van der Giessen (1992) proposed a method to integrate stresses for all loading cases. The principal Cauchy stresses $(\sigma_i)_{i=1,3}$ are given by

$$\sigma_i = -p + \frac{1}{4\pi} C_R\sqrt{N} \int_0^{\pi}\int_0^{2\pi} \mathscr{L}^{-1}\left(\frac{\lambda}{\sqrt{N}}\right) \lambda^4 m_i^2 \sin\theta \,\mathrm{d}\theta\,\mathrm{d}\phi, \tag{7}$$

where $C_R = nkT$, $m_1 = \sin\theta\cos\phi$, $m_2 = \sin\theta\sin\phi$, $m_3 = \cos\theta$ and

$$\lambda^{-2} = \sum_{i=1}^{3} \frac{m_i^2}{\lambda_i}. \tag{8}$$

The main advantage of this model is that it depends only on two physical parameters C_R and N that can be easily determined experimentally. This model agrees well with experiments for various deformation modes (Wu and van der Giessen, 1993). Nevertheless, the model suffers from the required numerical integration of the stress tensor. This difficulty does not permit its implementation in finite element codes because of excessive computing time.

2.2.2.3. p-chains models. Other authors used the non-Gaussian statistics theory to develop simpler models, which do not require numerical integration. Consider the unit sphere in Fig. 1 submitted to loading conditions. The density of polymer chains in the material is denoted n. Under loading, the sphere deforms into an ellipsoidal shape whose axes are the principal directions of the deformed continuum (see the four sub-figures in Fig. 1). The key feature of p-chains models is to restrict the complete integration to p privileged directions, assuming that n/p polymer chains per unit of volume are oriented in each of these directions in the undeformed state. Then, the previous integration of the strain energy is simply replaced by a sum of p single-chain strain energy functions weighted by the factor n/p.

The simplest p-chains model is defined by considering the three principal strain axes as privileged directions. Fig. 1(b) presents this three-chains model, which was derived by James and Guth (1943). The principal true stresses can be expressed as functions of the principal stretch ratios as

$$\sigma_i = -p + \frac{1}{3} C_R \sqrt{N} \lambda_i \mathscr{L}^{-1}\left(\frac{\lambda_i}{\sqrt{N}}\right). \tag{9}$$

Similarly, a four-chains model was developed by Flory (1944). The privileged directions are defined by the centre of the sphere and the vertices of the enclosed tetrahedron. They connect the centre of the tetrahedron with its vertices (see Fig. 1(c)). The stress–stretch relation cannot be expressed in a simple way because the position of the centre must be calculated for each particular deformation state. Moreover, this model gives similar results to the three-chains model. For these two reasons, it is not frequently used.

The more recent model based on this approach is the eight-chains model developed by Arruda and Boyce (1993). It is based on a unit cube enclosed in the unit sphere. The chain directions are defined by the half diagonals of the cube. Fig. 1(d) shows the geometry of the model. The major feature of this model is the symmetry of its geometry with respect to the three principal axes. Therefore, the eight chains are stretched with the same extension ratio $\lambda = \sqrt{I_1/3}$. This leads to a simple stress–stretch relationship:

$$\sigma_i = -p + \frac{1}{3} C_R \sqrt{N} \frac{\lambda_i^2}{\lambda} \mathscr{L}^{-1}\left(\frac{\lambda}{\sqrt{N}}\right). \tag{10}$$

Finally, we can mention the approximate full network model proposed by Wu and van der Giessen (1992), who used a linear combination of the stresses of the three-chains model (Eq. (9)) and of the eight-chains model (Eq. (10)) to approximate the full network stresses (Eq. (7)).

2.2.2.4. Comparison of chains models. In order to compare the accuracy of the previous models with experiments, Wu and van der Giessen (1993) considered the experimental data of James et al. (1975). They studied the three-chains, eight-chains and full network models by determining the material parameters C_R and N with uniaxial experimental data and comparing their respective accuracy using biaxial experimental data. Fig. 2 presents these results. As mentioned by Wu and van der Giessen, the eight-chains model predicts biaxial data more successfully than the two other models.

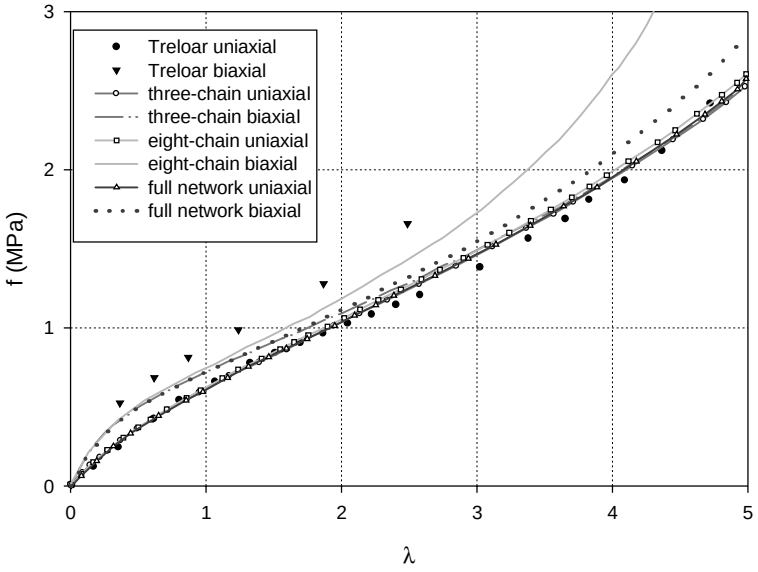

Fig. 2. Comparison of the full network, the three-chains and the eight-chains models.

Due to its relatively simple mathematical expression and its ability to reproduce different deformation modes with only two parameters, the Arruda–Boyce eight-chains model remains a good compromise to describe large strains of elastomers. It was successfully used for optics applications (von Lockette and Arruda, 1999) and structural mechanics (Allport and Day, 1996).

3. Previous works on the Mullins effect

3.1. Macroscopic considerations

The Mullins effect is considered as a damage mechanism of rubber material. It is characterized by a strain-induced stress softening of the material after a first load during loading cycles. Fig. 3 illustrates this phenomenon under quasi-static loading conditions. It shows the behaviour of an idealized material induced by the Mullins effect without visco-elastic phenomena and strain rate dependency. Let this material be subjected to an uniaxial strain history as shown in Fig. 3(a). The undamaged material is first stretched to the extension ratio λ_{I} and the stress follows the path denoted I in Fig. 3(b). Then the unloading from λ_{I} to 0 follows the path I$'$. The second loading, from 0 to $\lambda_{\mathrm{II}} > \lambda_{\mathrm{I}}$, first follows the path I$'$ until $\lambda = \lambda_{\mathrm{I}}$, then it follows path II. The second unloading, from the stretch ratio λ_{II} to 0, follows path II$'$, which is different from path I$'$. At a given stretch, the stress on II$'$ is lower than the stress on I$'$. Repeating this process, the loading path corresponding to the increase of stretch from 0 to λ_{III} is the path that

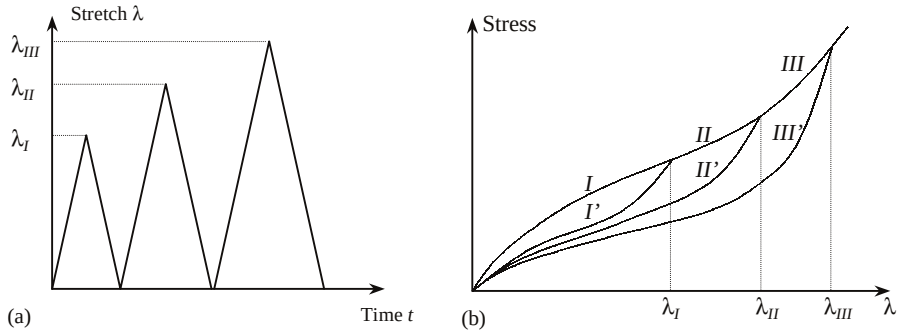

Fig. 3. Macroscopic description of the Mullins effect: (a) stretching history, (b) stress.

joins II′ and part III of the virgin curve. Finally, the corresponding unloading follows path III′. If the material is no longer stretched over the last maximum stretch λ_{III}, it will behave in an elastic manner and remains on path III′. For this reason the material is said to be pseudo-elastic.

From a historical point of view, this phenomenon was observed for the first time by Bouasse and Carrière (1903). It occurs in unfilled elastomers as well as in filled elastomers, though this effect is more pronounced in filled rubbers. Mullins and Tobin (1947) studied this phenomenon extensively. Moreover, it was demonstrated that rubbers recover partially or totally their original stiffness very slowly (after several days) at room temperature Mullins (1969). Nevertheless, Bueche (1960) and later Mullins (1969) observed that the stiffness recovery can be greatly accelerated by temperature: Bueche's experiments show that 50% of the stiffness is recovered after one hour at 100°C.

Another observation is pointed out by Mullins (1948) and James and Green (1975). They showed that the level of softening is not identical in all directions and that anisotropic stress–strain properties take place under stretching. The stress softening in the direction perpendicular to the stretch is less than half the softening observed in the direction of stretch.

3.2. Physical interpretations and constitutive modelling

There is no unanimous explanation of the physical causes of the Mullins effect in rubber-like materials.

Mullins and Tobin (1947) first developed a quantitative and phenomenological model, considering that the material is constituted by a soft phase and a hard phase. During deformation, hard regions are broken down and transformed into soft regions. Then the fraction of the soft region increases with increasing extension. Nevertheless, authors did not provide a direct physical interpretation for their model. More recently, Johnson and Beatty (1993) used the two-phases model of Mullins and Tobin and discussed physical justifications. They suggested that the hard phase of the model can be interpreted as clusters of molecular chains held together by short chain segments, entanglements or

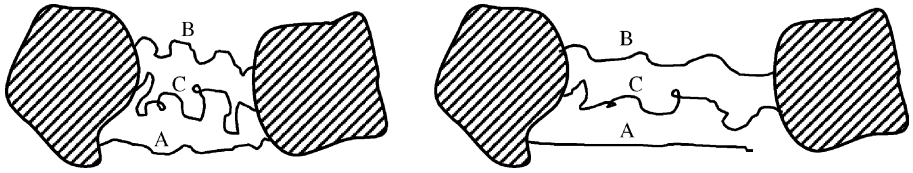

Fig. 4. Filler particle–chain junctions.

intermolecular forces. As the material is stretched, chains are pulled from clusters and hard regions are transformed into soft regions. Three phenomenological consequences are induced by this mechanism: first, the strain decreases in the soft region; second, the average chain length increases under loading; and finally, the hard phase is oriented in the stretching direction. This third consequence could explain the anisotropy of the material after softening.

Mullins (1969) suggested that the stress softening is due to a disentanglement of the network chains with the breakdown of interactions between the filler particles and the rubber matrix. A similar idea was suggested by Bueche (1960, 1961). For him, the main mechanism of the Mullins effect is the breakdown of links between filler particles and gum chains. The polymerization process leads to the formation of chains of different length between filler particles. Consider two filler particles joined together by different chains as shown in Fig. 4. Chains break down progressively as they reach their maximum extension: the chains A for λ_A, B for $\lambda_B > \lambda_A$ and C for $\lambda_C > \lambda_B$. Examining this situation, Bueche developed a probabilistic model of the contact between chains and filler particles that led to good agreement with experiments. A few years later, Harwood et al. (1967) suggested that the softening of the material occurs entirely in the rubber phase and that it is not the consequence of the breaking mechanism of gum–fillers interactions. Their observations lead to the conclusion that stress softening is primarily due to the rearrangement of the molecular network, involving displacement of network junctions. More recently, Govindjee and Simo (1991) also considered the ideas of Bueche, with the development of a free energy function for rubber matrix based on an averaging theory. They demonstrated that the generalization of their approach to a three-dimensional constitutive model presents major difficulties. Consequently, they concluded that an isotropic damage assumption is necessary. They also assumed that the principal directions remain constant in time. Nevertheless, their model gives good correlation with Bueche experimental data.

Moreover, Miehe (1995) and Ogden and Roxburgh (1999) proposed purely phenomenological models without providing physical interpretations for the Mullins effect. Miehe took into account discontinuous and continuous damage functions based on the classical damage mechanics, and Ogden and Roxburgh developed a constitutive equation in which the damage parameter is only active on the unloading parts of the loading history.

In the next section, a new model for the Mullins effect is presented. It is based on the above physical considerations and their corresponding effects on the material constitutive equation.

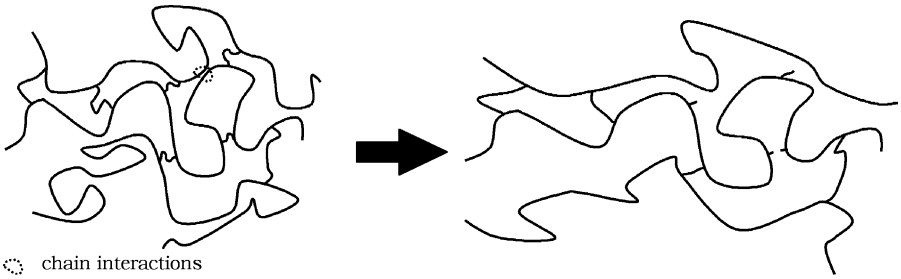

Fig. 5. Weak links and cross-links breakdown.

4. Application of the network alteration theory to the eight-chains model

4.1. Network alteration theory

In the present approach, the theory of links breakage inside the material is adopted without prejudging the nature of these links. The total or partial recovery of the stiffness with temperature suggests that, even if filler-matrix bonds are broken under loading, weak and recoverable interactions between polymer chains of the rubber matrix are also involved in the Mullins effect. Hence, the theory presented herein is consistent with the general feature of a rearrangement of the chains network under loading. The main consequence is an apparent increase in the average chain length as suggested by Johnson and Beatty (1993).

Indeed, consider the network configuration presented in Fig. 5. After polymerization, rubber chains are bonded at junction points, which are trivalent segment cross-links. Other links are weak molecular interactions due to the polarization of monomer molecules. These two types of links lead to an amorphous chains network, as shown in the left-hand side of Fig. 5. During stretching, some chains are extended until their limit of extensibility and chain breaking occurs. The number of breakdowns increases with the maximum stretch ratio of the continuum in which polymer chains are embedded. Moreover, this number of breakdowns highly depends on the distribution of the secondary bonds length (see the right-hand side of Fig. 5, especially grey zones). In the same way, some weak interactions are no more able to stand, and they break down during stretching. As the number of breakdowns increases, the number of junction points between chains decreases. Therefore, the average number of monomer segments in a polymer chain, previously denoted N, becomes larger. Using the previous developments, it is considered that N reduces to a function of the maximum stretching state endured by the material during its history.

Another consequence of the network rearrangement is a decrease of the chains density n. This is a consequence of the principle of mass conservation, which implies that the number of monomer segments per unit volume, Nn, must remain constant. Nevertheless, the conservation of mass must not be viewed in a strict manner in the present case. Monomer segments concerned by this principle are those which are involved in the stiffness of the material. During the alteration, some broken chains can

be transformed into dangling chains, which do not contribute to the material stiffness. So, theoretically, the product Nn may decrease. In the following parts, Nn is considered to remain constant.

The present theory can be related to the network alteration theory of Septanika and Ernst (1998a,b) used to model the time-dependent behaviour of rubbers. Their alteration process consists in the breakage of chains in the original network and the formation of new stress-free networks in the deformed state. At each time t_i, a new stress-free configuration C_i replaces a part of the previous configuration at time t_{i-1}. Then the breakage function of the initial undeformed configuration C_0 is represented by a relaxation function of the initial value of the chain density $n = n_0$. The newly formed configuration C_i is described by a formation function that depends on the chain density of this new configuration, said n_i. This theory gives good agreement with stress-relaxation experiments. In the present work, the Mullins effect is considered as an alteration process. Nevertheless, this alteration affects both the chain density n and the average number of segments N.

4.2. Modified constitutive equations using the network alteration theory

In order to incorporate the previous developments in classical hyperelastic constitutive equations, the simplest way consists in adapting one of the chains models. As these constitutive equations are expressed explicitly in terms of both physical parameters n and N, the integration of our alteration theory is quite obvious. Among these statistical models, the Arruda–Boyce eight-chains model (Eq. (10)) seems to be the best compromise. Indeed, it presents the advantages of being quite simple to derive, as compared to the full network model (Eq. (7)), and of giving better agreement with experimental data than the three-chains model (Eq. (9)). Another advantage of the eight-chains model is that it explicitly exhibits the average chain stretch ratio $\lambda = \sqrt{I_1/3}$. This stretch ratio can be used as the criterion that quantifies the maximum strain state endured during the history of the deformation. Note that the Mullins effect is classically described in terms of the maximum stretch ratio because of a lack of a well-defined criterion. Bergström and Boyce (1999) already used the chain stretch ratio as a measure to describe the strain amplification factor in elastomers hysteresis.

Thus, N and n are now written as follows:

$$N = N(\lambda_{\max}), \tag{11}$$

$$n = n(\lambda_{\max}) \tag{12}$$

with the condition

$$Nn = \text{constant}. \tag{13}$$

This criterion allows for the increase of softening during successive loadings in different directions without prejudging the loading path.

Then, the stress–strain relationship proposed here modifies the classical eight-chains model in Eq. (10) as

$$\sigma_i = -p + \frac{1}{3} C_R(\lambda_{max}) \sqrt{N(\lambda_{max})} \frac{\lambda_i^2}{\lambda} \mathscr{L}^{-1}\left(\frac{\lambda}{\sqrt{N(\lambda_{max})}}\right) \quad \text{for } i = 1,3, \tag{14}$$

where the parameter C_R is a function of the maximum chain stretch ratio:

$$C_R(\lambda_{max}) = n(\lambda_{max})\, kT. \tag{15}$$

In Eq. (14), the chain extension is defined by

$$\lambda(t) = \sqrt{I_1(t)/3}, \tag{16}$$

where t is the current time, and the maximum chain stretch ratio is

$$\lambda_{max} = \max_{0 \leqslant \tau \leqslant t} [\lambda(\tau)]. \tag{17}$$

In this paper, the assumption is made that the transformation is isothermal. Since the temperature appears in the expression of C_R (Eq. (15)), we assume that its evolution is only driven by the evolution of n and not of T.

In order to highlight the influence of the evolution of N on the mechanical behaviour, consider the uniaxial response of the classical Arruda–Boyce eight-chain model. The first Piola–Kirchhoff stress in the loading direction (denoted 1), i.e. the loading force per unit of undeformed area, can be written as

$$\pi_1 = \frac{C_R\sqrt{N}}{3\lambda} \mathscr{L}^{-1}\left(\frac{\lambda}{\sqrt{N}}\right)\left(\lambda_1 - \frac{1}{\lambda_1^2}\right). \tag{18}$$

This equation is obtained by determining the hydrostatic pressure p in Eq. (14) with the stress boundary conditions. Here, the initial stiffness C_R is set to a constant value (C_R=1.0) and all the constants are time-independent. Fig. 6 presents the response of the specimen for different values of the average number of segments in polymer chains, N. As N increases, the initial tangent stiffness decreases and the final asymptotic vertical line that represents the strain-hardening phenomenon is shifted to an increasing value of λ_{asympt}, which is a real solution of the following equation:

$$\lambda_{asympt}^2 + \frac{2}{\lambda_{asympt}} = 3N. \tag{19}$$

Now, the stress–strain diagram of Fig. 6 must be separated into two parts: the primary loading curve represented by the bold curve in the figure and the secondary loading curves. For the primary loading curve, the maximum chain stretch λ_{max} is equal to the current chain stretch, and consequently N evolves during the first load. For secondary curves, the maximum chain stretch remains constant until the curves intersect the primary loading curve. The corresponding average number of monomer segments in a chain is constant on each secondary curve. Thus, the primary curve can be considered as the master curve of every N-constant hyperelastic response, i.e. the classical Arruda–Boyce eight-chains stress–strain curves. The final difficulty resides in determining the function $N(\lambda_{max})$.

The study of the influence of $n(\lambda_{max})$ on mechanical response is straightforward. This parameter directly affects the stiffness of the material in a proportional manner.

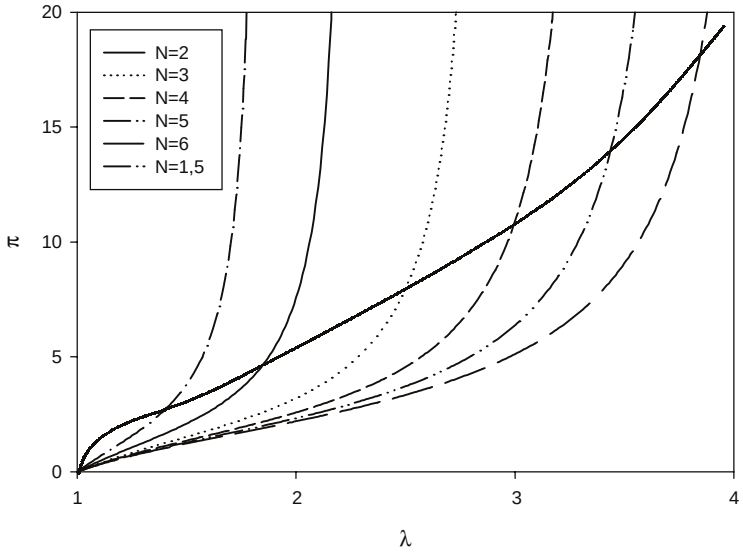

Fig. 6. Classical eight-chains model. Stress–strain response for different values of N.

In conclusion of this presentation of our theory, it is essential to recall the assumptions of the present approach. As mentioned previously, the present model does not include hysteretic and non-linear viscoelastic effects. It is restricted to quasi-static loading conditions. Moreover, as the model is written in terms of maximum chain stretches, the stress softening of the material is considered isotropic. The model is not able to account for some experimental observations that reveal that strain-softened rubbers become anisotropic (Mullins, 1948; Bonart, 1968). Finally, the present alteration network phenomenon considers that the Mullins effect is the result of micro-damages accumulation. Thus, in order to superpose these micro-damages for several loadings, constant stretching directions in time must be studied. Consequently, the present approach assumes that principal stretch directions remain constant.

4.3. Experiments

In order to validate the present approach, uniaxial stretching experiments are performed at room temperature. These uniaxial cyclic tests are conducted on flat coupon specimens under controlled strain. The specimens are 20 mm long, 4 mm large and 2.1 mm thick. For different strain levels, five loading cycles at constant strain rate $\dot{\lambda} = 0.05\ \mathrm{s}^{-1}$ are carried out. The elongation of the specimens is measured by a laser extensometer and the stretch ratio in the loading direction, called λ_1, is calculated with the assumption of homogeneous deformation. Moreover, we determine the first Piola–Kirchhoff stress, Π_1, as the axial force divided by the area of the undeformed specimen. The stress values are normalized by the maximum measured stress, so that stresses vary between 0. and 1. Fig. 7 shows the typical response of the specimen.

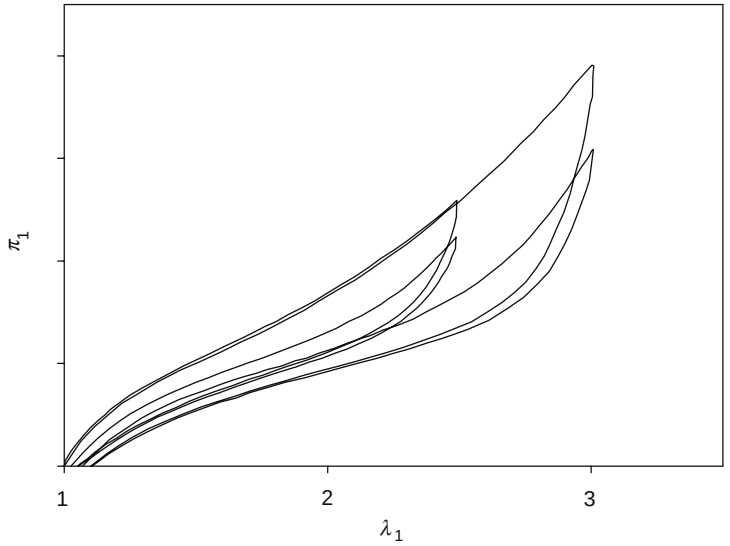

Fig. 7. Raw experimental data.

As the objective of the present work is the identification of the Mullins effect, the stress-softening effect has to be separated from other inelastic phenomena, such as hysteresis or viscous effects. Thus, experimental raw data are transformed by removing unloading parts (Chagnon et al., 2001) and secondary loading curves are shifted to zero on the abscissa axis to remove creep due to viscoelastic effects. Only the variation of stiffness in the loading and reloading paths is analysed, by assuming that the equilibrium curves follow the same evolution during the test. Thus, our approach is more qualitative than quantitative. A better way to identify the correct equilibrium curves would be to interrupt the load by relaxation periods during the loading and unloading in order to approach the equilibrium points, as proposed by Bergström and Boyce (1998). A time constraint in the use of the test device does not allow us to make the experiments in such a way. This could be remedied by constructing a more general constitutive model including time-dependent behaviour. Indeed, the model proposed by Bergström and Boyce (1998) is compatible with the present approach.

These experiments are conducted by one of the European Research Centers of Trelleborg. Two different materials are considered. The first one is a natural rubber, denoted NR through the rest of the paper. Its mass percentage of filler particles is approximately 25%. The second material is a SBR vulcanizate. The corresponding mass percentage of filler particles is about 40%.

4.4. Identification of material parameters

The identification method consists in minimizing the least-squares error between experimental and theoretical data. In order to investigate the evolution of both parameters C_R and N under mechanical loading, these parameters are approximated by empirical

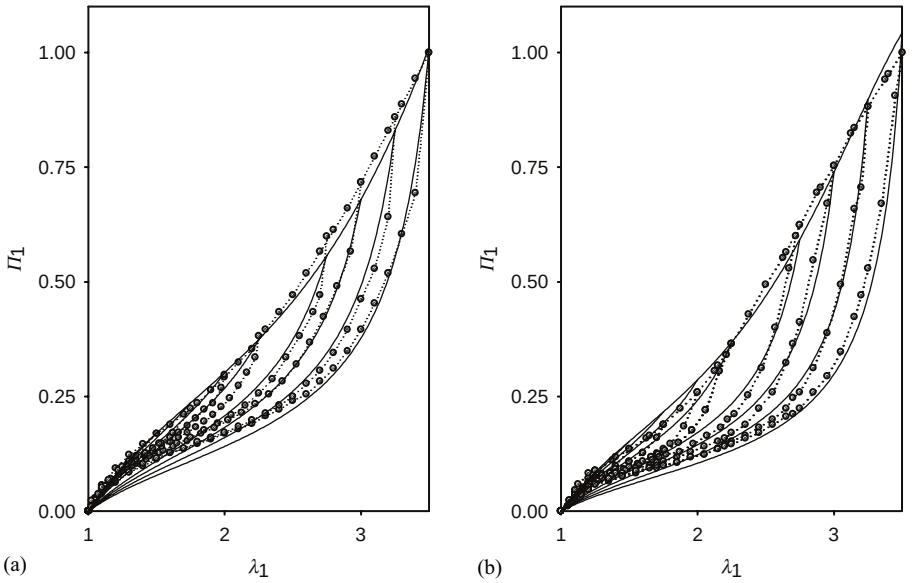

Fig. 8. Identification results, (a) NR and (b) SBR: (· · ·●· · ·) experiments, (—) our network alteration theory.

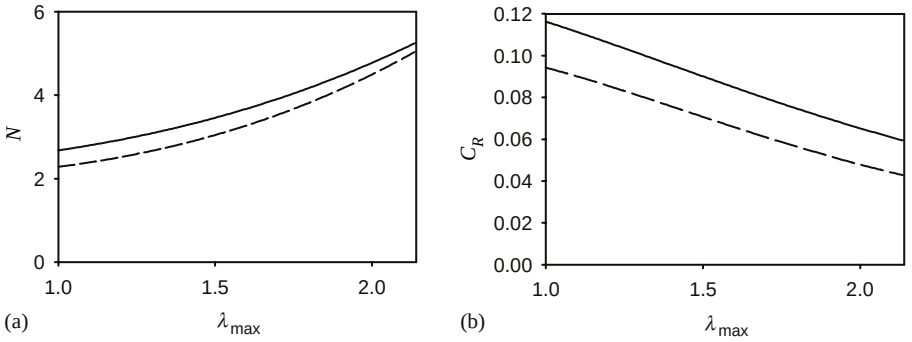

Fig. 9. Material parameters as a function of the maximum stretch ratio $\lambda_{\max}$, (a) N and (b) C_R: (—) NR, (- -) SBR.

polynomial functions that only depends on $\lambda_{\max}$. The degree of the polynomial functions can vary from 1 to 4 and it is determined by the identification program. The error is calculated simultaneously on all curves. Computations are performed using two different algorithms. First, an optimization program based on a genetic algorithm estimates approximately the material parameters. Second, these parameters are precisely determined with the help of a classical steepest descent algorithm using the genetic algorithm results as initial guess solutions.

The identification results obtained by the previous methods are compared with experiments in both Figs. 8 and 9. Before examining these results, one should note that our

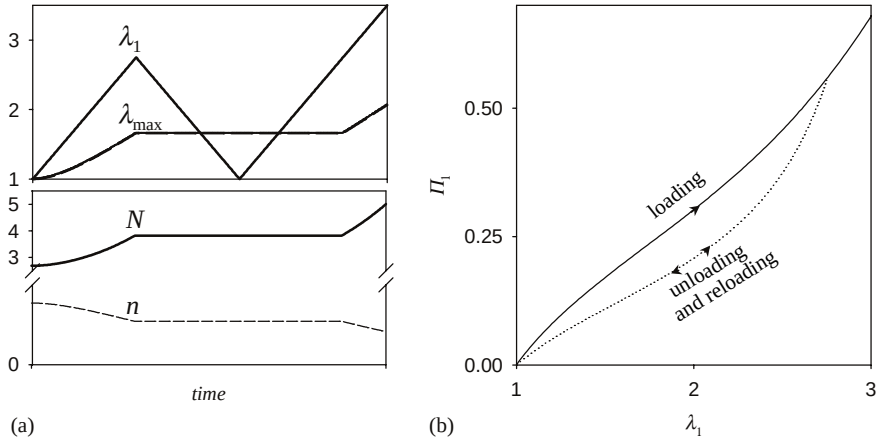

Fig. 10. Time evolution of the model parameters.

genetic algorithm yields several local minima: there is more than one set of optimized parameters. These different solutions exhibit similar qualitative behaviours. Therefore, we only focus on qualitative results, i.e., on the evolution of the parameters, rather than on their precise values.

Fig. 8 shows that our model agrees well with experimental data for both materials. Some discrepancies are observed at small strains. They are not due to our approach but are induced by the limitations of the eight-chains model that is known to have difficulty to reproduce rubber-like behaviour at small strains. This problem may be corrected, for example by using a modified phantom model as suggested by Boyce and Arruda (2000). The curves in Fig. 9 display the evolution of N and C_R as function of the maximum chain stretch ratio defined by Eq. (17). We observe that the results are highly similar for the two materials. As predicted by our network alteration theory, the stiffness parameter C_R decreases, i.e., the chain density n decreases as λ_{max} increases (see Fig. 9(b)). This observation agrees well with the conclusions of Septanika and Ernst (1998a). Moreover, the number of monomer segments per chain N increases as λ_{max} increases (see Fig. 9(a)). This result confirms our predictions.

Now, we describe the evolution of the parameters during a loop of loading, unloading and reloading. Fig. 10(a) shows the imposed value of λ as a function of time and the corresponding value of λ_{max} defined by Eq. (17). It can be seen that λ_{max} remains constant during unloading and reloading as long as λ is lower than λ_{max}, and then it increases again with λ. The lower sub-figure in Fig. 10(a) shows the evolution of the parameters N and n (i.e. C_R). The corresponding response of the material is illustrated by Fig. 10(b). The plain line shows the response to the first loading until the specimen stretch ratio λ_1 is 2.75. The dotted line shows the unloading and reloading elastic path until $\lambda_1 = 2.75$. When $\lambda_1 = 2.75$ for the second time, the slope of the response changes and the first loading curve is extended as if the specimen were stretch for the first time.

Finally, we examine the influence of filler particles on the mechanical behaviour. For the parameter N, the curves corresponding to both materials vary between similar

values. The main difference is their curvature: the curvature of the SBR N-function is greater than the curvature of the NR N-function (see Fig. 9(a)). The combination of these results leads to a more pronounced Mullins effect for the most filled material (SBR). This conclusion can be observed in Fig. 8 by examining areas limited by the primary loading curve and secondary loading curves.

5. Concluding remarks

A new statistical network constitutive equation for the Mullins effect has been proposed in this paper. The materials considered here are natural rubbers and synthetic elastomers. They are considered non-linear elastic, isotropic and incompressible, and viscous effects are not taken into account. The Mullins effect is considered as a consequence of chain–filler and chain–chain links breakage. It is demonstrated that the chain density and the average number of monomer segments in a chain are evolving during loading and depend on the maximum chain stretch ratio. Our theory has been incorporated into the classical eight-chains model, where the two classical material parameters C_R and N become functions of the maximum stretch ratio λ_{max}. Experimental uniaxial data are successfully reproduced by the model for two different materials.

From a numerical point of view, the proposed model only differs from the classical Arruda–Boyce model in the storage of the tracker λ_{max} and the evaluation of the constitutive parameters $N(\lambda_{max})$ and $n(\lambda_{max})$ (or $C_R(\lambda_{max})$) each time the stress or the stiffness of the material is computed. Consequently, implementation in finite element codes presents no major difficulties.

The present study leaves some issues off undamental importance unanswered. First, viscous effects should be considered and a non-linear viscoelastic constitutive equation must be derived. The combination of our approach with the recent viscoelastic network alteration theory of Septanika and Ernst (1998a) may be an interesting issue. Moreover, in our study the material functions are built using an empirical approach. Statistical developments based on the network physics could provide the form of these functions. Finally, a more complete experimental work is in progress to validate the model in different deformation modes such as biaxial extension and pure shear, and to investigate the material anisotropy induced by the Mullins effect.

Acknowledgements

The authors of the present article thanks the reviewers for their suggestions, which lead to a better formulation of the proposed model.

References

Allport, J.M., Day, A.J., 1996. Statistical mechanics material model for the constitutive modelling of elastomeric compounds. Proc. Inst. Mech. Engrs. Part C 210, 575–585.

Arruda, E., Boyce, M.C., 1993. A three-dimensional constitutive model for the large stretch behavior of rubber elastic materials. J. Mech. Phys. Solids 41 (2), 389–412.

Bergström, J.S., Boyce, M.C., 1998. Constitutive modeling of the large strain time-dependent behavior of elastomers. J. Mech. Phys. Solids 46 (5), 931–954.
Bergström, J.S., Boyce, M.C., 1999. Mechanical behavior of particule filled elastomers. Rubber Chem. Tech. 72, 633–656.
Bonart, R., 1968. X-ray investigations concerning the physical structure of cross-linking in segmented urethane elastomers. J. Macromol. Sci. Phys. Ed. B2, 115–138.
Bouasse, H., Carrière, Z., 1903. Courbes de traction du caoutchouc vulcanisé. Ann. Fac. Sciences de Toulouse 5, 257–283.
Boyce, M.C., Arruda, E.M., 2000. Constitutive models of rubber elasticity: a review. Rubber Chem. Technol. 73, 505–523.
Bueche, F., 1960. Molecular basis for the Mullins effect. J. Appl. Polym. Sci. 5 (10), 107–114.
Bueche, F., 1961. Mullins effect and rubber-filled interaction. J. Appl. Polym. Sci. 5 (15), 271–281.
Chagnon, G., Verron, E., Gornet, L., Marckmann, G., Charrier, P., Fort, P., 2001. Experimental identification and rheological modeling of the Mullins effect for carbon black-filled rubber. In: Proceedings of the Eighth Seminar on Elastomers, Le Mans, France, 8–12 May, pp. 79–82.
Doi, M., 1996. Introduction to Polymer Physics. Clarendon Press, Oxford.
Flory, P.J., 1944. Network structure and the elastic properties of vulcanized rubber. Chem. Rev. 35, 51–75.
Gent, A.N., Thomas, A.G., 1958. Forms of the stored (strain) energy function for vulcanized rubber. J. Polym. Sci. 28, 625–637.
Govindjee, S., Simo, J.C., 1991. A micro-mechanically based continuum damage model for carbon black-filled rubbers incorporating Mullins' effect. J. Mech. Phys. Solids 39 (1), 87–112.
Hart-Smith, L.J., 1966. Elasticity parameters for finite deformations of rubber-like materials. Z. Angew. Mathe. Phys. 17, 608–626.
Harwood, J.A.C., Mullins, L., Payne, A.R., 1967. Stress softening in rubbers—A review. J. IRI 1, 17–27.
James, A.G., Green, A., 1975. Strain energy functions of rubber. II. Characterization of filled vulcanizates. J. Appl. Polym. Sci. 19, 2319–2330.
James, H.M., Guth, E., 1943. Theory of the elastic properties of rubber. J. Chem. Phys. 11 (10), 455–481.
James, A.G., Green, A., Simpson, G.M., 1975. Strain energy functions of rubber. I. characterization of gum vulcanizates. J. Appl. Polym. Sci. 19, 2033–2058.
Johnson, M.A., Beatty, M.F., 1993. The Mullins effect in uniaxial extension and its influence on transverse vibration of rubber string. Continuum Mech. Thermodyn. 5, 83–115.
Kuhn, W., Gr ün, F., 1942. Beziehungen zwichen elastischen konstanten und dehnungsdoppelbrechung hochelastischer stoffe. Kolloideitschrift 101, 248–271.
Lion, A., 1998. Thixotropic behavior of rubber under dynamic loading histories: Experiments and theory. J. Mech. Phys. Solids 46 (5), 895–930.
Miehe, C., 1995. Discontinuous and continuous damage evolution in Ogden-type large-strain elastic materials. Eur. J. Mech. A =Solids 14 (5), 697–720.
Mooney, M., 1940. A theory ofl arge elastic deformation. J. Appl. Phys. 11, 582–592.
Mullins, L., 1948. Effect of stretching on the properties of rubber. Rubber Chem. Technol. 21, 281–300.
Mullins, L., 1969. Softening of rubber by deformation. Rubber Chem. Technol. 42, 339–362.
Mullins, L., Tobin, N.R., 1947. Theoretical model for the elastic behavior of filler-reinforced vulcanized rubbers. Rubber Chem. Technol. 30, 551–571.
Ogden, R.W., 1972. Large deformation isotropic elasticity—on the correlation of theory and experiment for incompressible rubberlike solids. Proc. R. Soc. London A 326, 565–584.
Ogden, R.W., Roxburgh, D.G., 1999. A pseudo-elastic model for the Mullins effect in filled rubber. Proc. R. Soc. London A 455, 2861–2877.
Rivlin, R.S., Saunders, D.W., 1951. Large elastic deformations ofi sotropic materials—VII. Experiments on the deformation of rubber. Philos. Trans. R. Soc. A 243, 251–288.
Septanika, E.G., Ernst, L., 1998a. Application of the network alteration theory for modeling the time-dependent behavior of rubber. Part I. General theory. Mech. Mater. 30, 253–263.
Septanika, E.G., Ernst, L., 1998b. Application of the network alteration theory for modeling the time-dependent behavior of rubber. Part II. Experimental verification. Mech. Mater. 30, 265–273.
Treloar, L.R.G., 1943. The elasticity of a network ofl ong chain molecules (1 and 2). Trans. Faraday Soc. 39, 36–64, 241–246.

Treloar, L.R.G., 1975. Physics of Rubber Elasticity, 3rd Edition. University Press, Oxford.
Treloar, L.R.G., 1976. The mechanics of rubber elasticity. Proc. R. Soc. London A 351, 301–330.
Treloar, L.R.G., Riding, G., 1979. A non-gaussian theory for rubber in biaxial strain. I. Mechanical properties. Proc. R. Soc. London A 369, 261–280.
Valanis, K.C., Landel, R.F., 1967. The strain-energy function of a hyperelastic material in terms of the extension ratios. J. Appl. Phys. 38 (7), 2997–3002.
von Lockette, P.R., Arruda, E.M., 1999. A network description of non-gaussian stress-optic and raman scattering responses of elastomer networks. Acta Mech. 134, 81–107.
Wu, P.D., van der Giessen, E., 1992. On improved 3-D non-gaussian network models for rubber elasticity. Mech. Res. Commun. 19 (5), 427–433.
Wu, P.D., van der Giessen, E., 1993. On improved 3-D non-gaussian network models for rubber elasticity and their applications to orientation hardening in glassy polymers. J. Mech. Phys. Solids 41 (3), 427–456.